CRYSTAL GROWTH & DESIGN

Article

pubs.acs.org/crystal

Clues from Crystal Structures Pave the Way to Access Chiral *myo*-Inositol Derived Versatile Synthons: Resolution of Racemic 4-*O*-Allyl-*myo*-Inositol-1,3,5-Orthoesters via Corresponding Dicamphanates by Crystallization

Nivedita T. Patil,[†,‡] Mysore S. Shashidhar,*[,†,‡] Majid I. Tamboli,[‡] and Rajesh G. Gonnade*[,†,§]

[†]Academy of Scientific and Innovative Research (AcSIR), Anusandhan Bhawan, 2 Rafi Marg, New Delhi 110001, India

[‡]Division of Organic Chemistry and [§]Center for Materials Characterization, CSIR-National Chemical Laboratory, Pashan Road, Pune 411008, India

Supporting Information

ABSTRACT: Racemic 4-*O*-allyl-*myo*-inositol-1,3,5-orthoesters were resolved as the corresponding diastereomeric dicamphanates by crystallization from alcoholic solvents. Crystals of the two diastereomers of *myo*-inositol orthoacetate and one diastereomer each of *myo*-inositol orthoformate and *myo*-inositol orthobenzoate were obtained in >99% purity, on gram scale. The configuration of all these diastereomers was established by conversion to known chiral *myo*-inositol derivatives as well as by single crystal structure analysis. It is interesting to note that the procedures for the separation of diastereomeric *myo*-inositol orthoesters could be evolved due to the knowledge of crystal growth and crystal structures of inositol derivatives of comparable molecular structures. Due to the synthetic versatility of *myo*-inositol orthoesters, the methods described provide rapid and convenient access to a variety of chiral inositol derivatives with high synthetic potential.

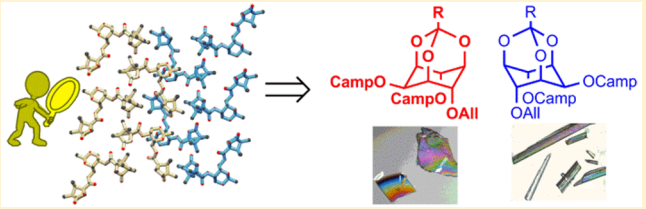

INTRODUCTION

Since the discovery of the relationship between intracellular concentrations of phosphoinositols and the release of calcium ions from intracellular sources, the chemistry and biology associated with naturally occurring inositol derivatives has expanded into a contemporary area of research with brisk activity.[1−4] Orthoesters of *myo*-inositol have been extensively used as early intermediates for the synthesis of phosphoinositols,[5] cyclitols and their derivatives,[6−9] metal complexing agents,[10,11] and natural products containing the cyclitol moiety.[12,13] Considerable efforts have been invested in obtaining chiral *myo*-inositol derivatives from these rigid symmetric triols, since they can be obtained in gram quantities swiftly from commercially available *myo*-inositol. *myo*-Inositol has the *meso*-configuration and hence preparation of chiral *myo*-inositol derivatives necessarily involves the destruction of its symmetry. The six secondary hydroxyl groups of *myo*-inositol have subtle differences in reactivity. These aspects dictate the use of elaborate separation and resolution procedures, often resulting in the isolation of (at best) less than gram quantities of enantiomeric inositol derivatives. We are interested in developing practical methods for the preparation of chiral *myo*-inositol derivatives (starting from *myo*-inositol) that could be used as early intermediates for the synthesis of cyclitol derivatives including natural products. Herein we reveal the separation of diastereomeric dicamphanates of racemic 4-*O*-allyl-*myo*-inositol-1,3,5-orthoesters (on grams scale) by crystallization. This process could be realized due to our past association with crystallization and crystal structures of inositol derivatives.,[14−21] Crystallization, although an enigmatic process, is perhaps the oldest method of separation and purification of organic compounds and provides synthetic intermediates ranging from milligram to kilogram scale in a short time. Crystallization as a method of separation and purification is also environmentally sustainable since solvents used can easily be recovered and recycled.

EXPERIMENTAL SECTION

Synthesis of Racemic 4-*O*-Allyl-*myo*-inositol-1,3,5-orthoacetate (4). *myo*-Inositol-1,3,5-orthoacetate (**1**, 2.212 g, 10.8 mmol) was dissolved in dry DMF (30 mL). To the ice cooled solution, sodium hydride was added (0.434 g, 10.8 mmol) with stirring. After 10−15 min allyl bromide (1.3 mL, 13.0 mmol) was added dropwise with stirring. The reaction mixture was stirred overnight (8−10 h) and quenched by the addition of ice, and DMF was removed under reduced pressure. The residue was worked up as usual. The crude product was purified by column chromatography (100−200 mesh silica gel, eluent 1:4 ethyl acetate:light petroleum) to obtain **4** as a gum (1.900 g, 72%). R_f = 0.4 (1:1 ethyl acetate:light petroleum), IR ($CHCl_3$) $\bar{\nu}$ = 3200−3500 cm^{-1}, ^1H NMR (200 MHz, Chloroform-*d*) δ 1.45 (s, 3 H), 3.26 (d, J = 11.6 Hz, 1 H D_2O ex.), 3.66 (d, J = 10.1 Hz, 1 H, D_2O ex.), 3.95−4.05 (m, 1 H), 4.11−4.51 (m, 7 H), 5.24−5.40 (m, 2 H), 5.77−6.00 ppm (m, 1 H), ^{13}C NMR (101 MHz,

Received: June 26, 2017
Revised: August 18, 2017
Published: August 24, 2017

DOI: 10.1021/acs.cgd.7b00895
Cryst. Growth Des. XXXX, XXX, XXX−XXX

Chloroform-*d*) δ 24.1, 59.7, 67.3, 67.6, 71.8 (CH_2), 72.7, 73.9, 75.2, 108.6, 119.4 (CH_2), 132.7 ppm, HRMS $[C_{11}H_{16}O_6+ H]^+$ (245.1020), found 245.1019.

Acylation of Racemic 4-*O*-Allyl-*myo*-inositol-1,3,5-orthoacetate (4) with Camphanic Acid Chloride: Procedure [A]. The racemic orthoacetate **4** (1.7 g, 6.9 mmol), dry dichloromethane (10 mL), triethylamine (10 mL), DMAP (0.250 g), pyridine (10 mL), and (1*S*)-(−)-camphanic acid chloride (3.77 g, 17.4 mmol) were refluxed (80−85 °C) for 48 h in an inert atmosphere. The reaction mixture was quenched by adding few pieces of ice, concentrated, and worked up in dichloromethane (500 mL) as usual. The product was purified by column chromatography (silica gel 60−120 mesh, eluent: 1:4 ethyl acetate:light petroleum) to obtain the mixture of diastereomers **7** and **dia7** as a gum (4.00 g, 95%). R_f **dia7** = 0.45, R_f **7** = 0.4 (3:17 ethyl acetate:light petroleum, five runs), IR ($CHCl_3$) $\bar{\nu}$ = 1756, 1790 cm^{-1}, ^1H NMR (200 MHz, Chloroform-*d*) δ 0.94−1.03 (3s, 6 H), 1.04−1.18 (5s, 12 H), 1.45 (s, 3 H), 1.60−1.79 (m, 2 H), 1.80−2.21 (m, 4 H), 2.29−2.62 (m, 2 H), 4.00−4.16 (m, 2 H), 4.25−4.48 (m, 3 H), 4.50−4.60 (m, 1 H), 5.15−5.38 (m, 3 H), 5.43−5.60 (m, 1 H), 5.75−6.02 ppm (m, 1 H); ^{13}C NMR (101 MHz, Chloroform-*d*) δ 9.6, 9.65, 9.67, 16.54, 16.63,16.65, 16.9, 24.0, 28.74(CH_2), 28.8(CH_2), 28.9(CH_2), 29.0(CH_2), 30.48(CH_2), 30.52(CH_2), 30.56(CH_2), 30.8(CH_2), 54.16, 54.26, 54.39, 54.45, 54.75, 64.0, 67.0, 67.3, 68.7, 69.0, 69.3, 69.7, 70.1, 71.3(CH_2), 71.6(CH_2), 72.5, 72.7, 90.7, 90.8, 90.86, 90.92, 109.1, 118.88(CH_2), 118.96(CH_2), 133.5, 133.6, 166.2, 166.7, 166.8, 166.9, 177.64, 177.7, 177.8, 177.85 ppm, Elemental analysis: calculated for $C_{31}H_{40}O_{12}$ (604.65); C, 61.58%; H, 6.67%; found, C, 61.45%; H, 6.64%.

The diastereomeric mixture (0.500 g) was column chromatographed (silica gel 230−400 mesh, 1:9 ethyl acetate: light petroleum) to obtain enriched (about 1:4 as revealed by ^1H NMR spectroscopy) mixture of diastereoisomers **A** (0.150 g) and **B** (0.110 g). The enriched sample **A** (0.120 g) was crystallized from hot absolute ethanol (5 mL) when crystals of **dia7** were obtained (0.040 g, 58% from enriched sample **A**). A similar crystallization procedure (in ethanol) with **B** (0.100 g) provided the solvated crystals of the **7**·EtOH (0.045 g, 45%). The crystals of the individual diastereomers **dia7** and **7**·EtOH obtained were subsequently used as seed crystals to separate the mixture of the diastereoisomers on larger scale.

Acylation of Racemic 4-*O*-Allyl-*myo*-inositol-1,3,5-orthoacetate (4) with (1*S*)-(−)-Camphanic Chloride. Procedure [B]. To a cooled mixture of the racemic **4** (5.100 g, 20.9 mmol), dry dichloromethane (30 mL), dry triethylamine (25 mL), dry pyridine (25 mL), and DMAP (0.750 g), (1*S*)(−) camphanic acid chloride (11.31 g, 52.2 mmol) was added and the mixture refluxed for 48 h in an argon atmosphere. After usual workup and chromatography a mixture of diastereomers **7** and **dia7** (12.0 g, 95%) was isolated by column chromatography (silica gel 60−120 mesh, eluent: 1:4 ethyl acetate:light petroleum).

Crystallization Procedure [B1]. The mixture of diastereomers **7**, **dia7** (gum, 10.0 g) obtained as above was taken in a 1 L round-bottom flask and dissolved in ethanol (75−100 mL) by warming. Seed crystals of **7**·EtOH were added and the flask was stored at room temperature (open to atmosphere) for 1−3 days when very thin needles or blocks of **7**·EtOH appeared. These crystals were filtered (3.5 g, purity 99%). [Storage of the ethanol solution (as above) for longer period of time resulted in the deposition of an amorphous solid **dia7** on crystals of **7**·EtOH that had appeared previously.] The mother liquor was concentrated to a gum and dissolved in warm ethanol (40−60 mL) and the clear solution was allowed to attain room temperature. The seed crystals of the **dia7** (obtained on 0.5 g scale as above) were added and stored (open to atmosphere) at room temperature for 1−3 days when **dia7** appeared as fibrous thin needle shaped crystals or an amorphous solid (1.2 g, purity 99%). The residue obtained from the mother liquor on crystallization using seed crystals of **7**·EtOH gave crystals of **7**·EtOH (1 g). These crystals were recrystallized form ethanol to obtain **7**·EtOH (0.95 g) of purity 99%. The residue obtained from the mother liquor on crystallization using seed crystals of **dia7** gave an additional quantity of **dia7** (2.2 g), which was recrystallized from ethanol. Thus, by repetitive crystallization using the two diastereomers as seed crystals alternately, **7**·EtOH (4.5 g, 45%) and **dia7** (4.0 g, 40%) could be separated efficiently with a purity of 99%.

Data for 7·EtOH. M.P. = 115 °C (Crystals from ethanol **7**·EtOH = 2:1), IR (Nujol) $\bar{\nu}$ = 1750, 1792 cm^{-1}, $[\alpha]_D^{rt}$ = +6.8 [$CHCl_3$, *c* = 1.0], ^1H NMR (400 MHz, Chloroform-*d*) δ 0.99 (s, 3 H), 1.00 (m, 3 H), 1.09 (m, 3 H), 1.11 (m, 3 H), 1.14 (s, 6H), 1.24 (t, *J* = 7 Hz, 2 H, Ethanol) 1.45 (s, 3 H), 1.64−1.77 (m, 2 H), 1.86−2.15 (m, 4 H), 2.37−2.54 (m, 2 H), 3.71 (q, *J* = 7.1 Hz,1 H, Ethanol), 4.02−4.13 (m, 2 H), 4.29 (br. s., 1 H), 4.35−4.39 (m, 2 H), 4.55 (br. s., 1 H), 5.20 (s, 1 H), 5.23−5.35 (m, 2 H), 5.53−5.58 (m, 1 H), 5.80−6.00 (m, 1 H) ppm, ^{13}C NMR (101 MHz, Chloroform-*d*) δ 9.64, 9.68, 16.58, 16.63, 16.69, 16.94, 18.4(CH_3, Ethanol), 24.0, 28.9 (CH_2), 29.0 (CH_2), 30.57 (CH_2), 30.62 (CH_2), 54.2, 54.5, 54.8, 58.5 (CH_2, Ethanol), 64.1, 67.0, 68.8, 69.1, 70.2, 71.6 (CH_2), 72.8, 90.8, 90.9, 109.1, 119.0 (CH_2), 133.5, 166.2, 167.0, 177.66, 177.70 ppm, Elemental analysis: calculated for $C_{31}H_{40}O_{12}$0.5 EtOH (627.65); C, 61.23%; H, 6.91%; found, C, 60.95%; H, 6.91%.

Data for dia7. M.P. = 160 °C (crystals from ethanol), IR (Nujol) $\bar{\nu}$ = 1745, 1789 cm^{-1}; $[\alpha]_D^{rt}$ = −19.28 [$CHCl_3$, *c* = 1.0], ^1H NMR (500 MHz, Chloroform-*d*) δ 1.00 (s, 3 H), 1.01 (s, 3 H), 1.07 (s, 3 H), 1.11 (s, 3 H), 1.12 (s, 3 H), 1.14 (br s, 3 H), 1.45 (s, 3 H), 1.65−1.77 (m, 2 H), 1.87−2.00 (m, 2 H), 2.01−2.15 (m, 2 H), 2.35−2.45 (m, 1 H), 2.46−2.55 (m, 1H) 4.06−4.15 (m, 2 H), 4.29 (br. s., 1 H), 4.39−4.46 (m, 2 H), 4.55 (br s, 1 H), 5.18 (s, 1 H), 5.23−5.35 (m, 2 H), 5.46−5.52 (m, 1 H), 5.84−5.95 ppm (m, 1 H); ^{13}C NMR (126 MHz, Chloroform-*d*) δ 9.68, 9.74, 16.6, 16.7, 24.1, 28.8(CH_2), 29.0(CH_2), 30.6(CH_2), 30.8(CH_2), 54.3, 54.5, 54.8, 64.1, 67.4, 69.34, 69.35, 69.8, 71.3(CH_2), 72.6, 90.7, 91.0, 109.2, 118.9(CH_2), 133.7, 166.8, 166.9, 177.86, 177.91 ppm, Elemental analysis: calculated for $C_{31}H_{40}O_{12}$ (604.65); C, 61.58%; H, 6.67%; found, C, 61.56%; H, 6.76%.

Preparation of 1*D*-(−)-4-*O*-allyl-*myo*-inositol-1,3,5-orthoacetate (ent12). A mixture of **dia7** (1.000 g, 1.5 mmol), MeOH (20 mL), dichloromethane (20 mL), and *iso*-butyl amine (10 mL) was refluxed overnight (10−12 h), in an inert atmosphere. The solvent was removed under reduced pressure and the gummy residue was dissolved in ethyl acetate and worked up as usual. The product was purified by column chromatography (silica gel, 100−200 mesh, eluent 3:7 ethyl acetate:light petroleum) to get **ent12** (0.370 g, 92%) as a gum. R_f: 0.4 (1:1ethyl acetate: light petroleum), $[\alpha]_D^{rt}$ = −25 ($CHCl_3$, *c* = 1.5), IR (Neat) $\bar{\nu}$ = 3450−3550 cm^{-1}, ^1H NMR (400 MHz, $CDCl_3$) δ 1.45 (s,3H), 3.36 (br s, 1 H, D_2O exchangeable), 3.66 (br s, 1 H, D_2O exchangeable), 4.0 (s, 1 H), 4.09−4.18 (m, 2 H), 4.20−4.23 (m, 1 H), 4.24−4.26 (m, 1 H), 4.27−4.31 (m, 1 H), 4.32−4.36 (m, 1 H), 4.42 (br s, 1 H), 5.27−5.35 (m, 2 H), 5.82−5.94 ppm (m, 1 H); ^{13}C NMR (101 MHz, $CDCl_3$) δ 24.0, 59.6, 67.3, 67.5, 71.7(CH_2), 72.7, 73.9, 75.2, 108.5, 119.3(CH_2), 132.7 ppm, HRMS $[C_{11}H_{16}O_6+H]^+$ (245.1020), found 245.1022.

Preparation of 1*D*-(−)-2,6-di-*O*-benzyl *myo*-inositol-1,3,5-orthoacetate (ent13). The diol **ent12** (0.260 g, 1.1 mmol), was dissolved in dry DMF (4 mL). To the cold solution, sodium hydride (0.130 g, 3.2 mmol) was added and the reaction mixture was stirred for 10−15 min. To this mixture benzyl bromide (0.52 mL, 4.3 mmol) was added dropwise. The reaction mixture was stirred for 14 h at room temperature. The reaction mixture was quenched by the addition of few pieces of ice and DMF was removed under reduced pressure. The residue was worked up as usual using ethyl acetate to obtain the gummy residue. The gummy residue obtained (0.208 g, 0.4 mmol) was dissolved in the *iso*-propanol (3 mL) and refluxed for 4−5 h after the addition of 20% palladium hydroxide (0.130 g, 0.3 mmol). The reaction mixture was filtered through Celite bed. The bed was washed with methanol and ethyl acetate. The filtrate was concentrated under reduced pressure. The residue was column chromatographed (silica gel 60−120 mesh, eluent, 1:4 ethyl acetate:light petroleum) to isolate **ent13** as a gum (0.155 g, 88% over two steps). R_f = 0.35 (1:4 ethyl acetate:light petroleum), $[\alpha]_D^{rt}$ = -8.4 ($CHCl_3$, *c* = 1.0), IR ($CHCl_3$) $\bar{\nu}$ = 3450−3550 cm^{-1}; ^1H NMR (400 MHz, $CDCl_3$) δ 1.46 (s, 3 H), 3.51 (d, *J* = 9.8 Hz, 1 H, D_2O exchangeable), 3.81 (s, 1 H), 4.16−4.20 (m, 1 H), 4.24−4.28 (m, 1 H), 4.29−4.32 (m, 1 H), 4.32−4.36 (m, 1 H), 4.36−4.40 (m, 1 H), 4.41−4.51 (m, 2 H), 4.59−4.67 (m, 1 H),

DOI: 10.1021/acs.cgd.7b00895
Cryst. Growth Des. XXXX, XXX, XXX−XXX

Scheme 1. Conversion and Separation of Racemic 4-*O*-Allyl-*myo*-inositol-1,3,5-orthoesters to the Corresponding Diastereomeric Dicamphanates[a]

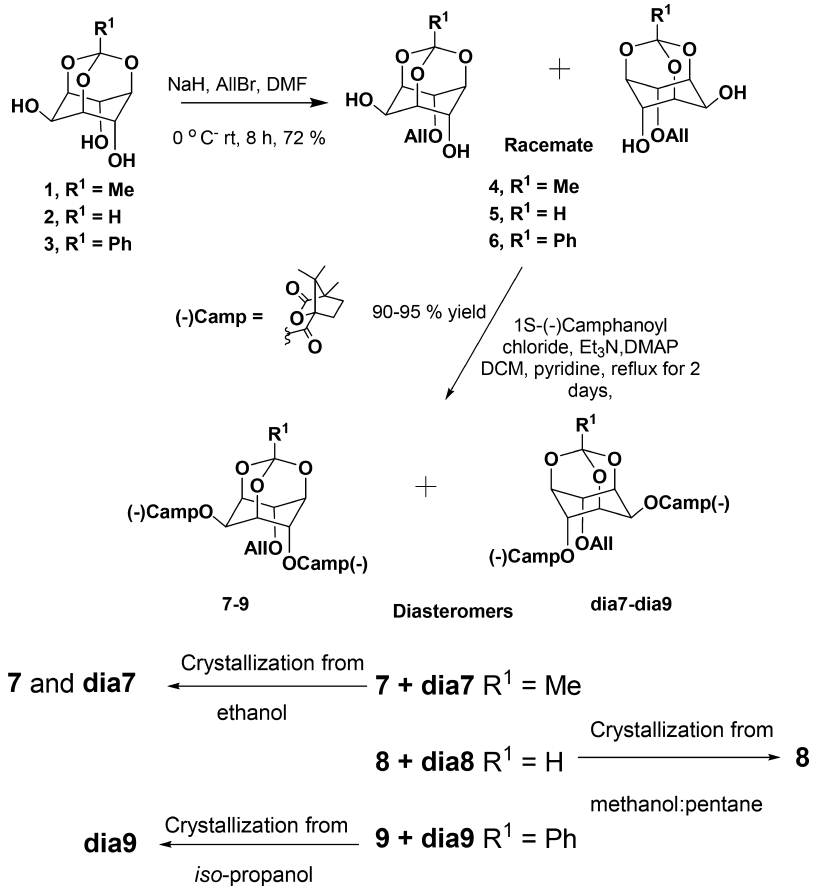

[a]Yield of crystals with diastereomeric purity >99% were **7**·EtOH (45%), **dia7** (40%), **8** (43%) for 10 g scale, **dia9** (20%) for 5 g scale (SI, S4–S10).

4.72–4.79 (m, 1 H), 7.12–7.19 (m, 2 H), 7.31–7.44 ppm (m, 8 H); ^{13}C NMR (101 MHz, $CDCl_3$) δ 24.1, 64.9, 67.7, 67.9, 70.5, 71.0(CH_2), 72.66(CH_2), 72.67, 74.3, 108.4, 127.86, 127.92, 128.4, 128.6, 128.7, 135.9, 137.6 ppm; HRMS $[C_{22}H_{24}O_6+H]^+$ (385.1646), found 385.1649.

Preparation of 1*D*-(−)-2,6-di-*O*-benzyl-*myo*-inositol (ent14). The orthoacetate **ent13** (0.150 g, 0.16 mmol) was dissolved in a mixture of methanol (3 mL) and 5 M aqueous HCl (1 mL) and refluxed for 16 h. The solvents were removed under reduced pressure and the crude product was purified by column chromatography (by washing the column with ethyl acetate) to isolate the known **ent14** as a solid (0.130 g, 93%).[22] M.P. 140 °C (crystals obtained from the *iso*-propanol) Lit. M.P. 145 °C HPLC analysis showed the enantiomeric purity to be >99%. R_f = 0.3 (ethyl acetate), Found $[\alpha]_D^{rt}$ (EtOH, *c* = 1.0) = −29.4; Lit. $[\alpha]_D^{rt}$ (EtOH, *c* = 1.0) = −29.9.[22]

Preparation of 1*D*-(+)-6-*O*-allyl-*myo*-inositol-1,3,5-orthoacetate (12). A mixture of 7·EtOH (1.00 g, 1.45 mmol), methanol (20 mL), dichloromethane (20 mL), and *iso*-butyl amine (10 mL) was refluxed overnight (10–12 h), in an inert atmosphere. The solvent was removed under reduced pressure and the gummy residue was dissolved in ethyl acetate and worked up as usual. The product was purified by column chromatography (silica gel, 100–200 mesh, eluent 3:7 ethyl acetate:light petroleum) to get **12** (0.348 g, 98%) as a gum. R_f = 0.4 (1:1 ethyl acetate:light petroleum), $[\alpha]_D^{rt}$ = +25.24 ($CHCl_3$, *c* = 1.5); ^{1}H NMR (400 MHz, $CDCl_3$) δ 1.43 (s, 3 H), 3.25 (br s, 1 H), 3.64 (br s, 1 H), 3.98 (s, 1 H), 4.07–4.17 (m, 2 H), 4.17–4.34 (m, 4 H), 5.19–5.36 (m, 2 H), 5.86 (dq, *J* = 5.8, 11.1 Hz, 1 H); ^{13}C NMR (101 MHz, $CDCl_3$) δ 24.0, 59.6, 67.3, 67.5, 71.7(CH_2), 72.7, 73.9, 75.2, 108.5, 119.3(CH_2), 132.7 ppm, HRMS $[C_{11}H_{16}O_6+H]^+$ (245.1020), found 245.1020.

Preparation of 1*D*-(+)-2,4-di-*O*-benzyl-*myo*-inositol-1,3,5-orthoacetate (13). The diol **12** (0.260 g, 1.06 mmol), was dissolved in the dry DMF (5 mL). To the cold solution, sodium hydride (0.130 g, 3.18 mmol) was added and the mixture was stirred for 10–15 min. To this mixture benzyl bromide (0.52 mL, 4.3 mmol) was added dropwise. The reaction mixture was stirred for 14 h at room temperature. The reaction was quenched by addition of few pieces of ice and DMF was removed under reduced pressure. The residue was worked up as usual using ethyl acetate to obtain gummy residue. The gummy residue obtained was dissolved in the *iso*-propanol (3 mL) and refluxed for 4–5 h after the addition of 20% palladium hydroxide (0.070 g). The reaction mixture was filtered through Celite bed. The Celite bed was washed with methanol and ethyl acetate. The filtrate was concentrated under reduced pressure. The residue was column chromatographed (silica gel 60–120 mesh, eluent, 1:4 ethyl acetate:light petroleum) to isolate **ent13** as a gum (0.155 g, 88% over two steps). R_f = 0.35 (1:5 ethyl acetate:light petroleum), $[\alpha]_D^{rt}$ = +8.9 ($CHCl_3$, *c* = 1.0); ^{1}H NMR (400 MHz, $CDCl_3$) δ 1.46 (s, 3 H), 3.51 (d, *J* = 9.8 Hz, 1 H, D_2O exchangeable), 3.81 (s, 1 H), 4.16–4.20 (m, 1 H), 4.24–4.28 (m, 1 H), 4.29–4.32 (m, 1 H), 4.32–4.36 (m, 1 H), 4.36–4.42 (m, 1 H), 4.42–4.51 (m, 2 H), 4.59–4.67 (m, 1 H), 4.72–4.79 (m, 1 H), 7.12–7.19 (m, 2 H), 7.31–7.44 ppm (m, 8 H); ^{13}C NMR (101 MHz, $CDCl_3$) δ 24.1, 64.9, 67.7, 67.9, 70.5, 71.0(CH_2), 72.66(CH_2), 72.67, 74.3, 108.4, 127.9, 128.4, 128.6, 128.7, 135.9, 137.6 ppm, HRMS $[C_{22}H_{24}O_6+H]^+$ (385.1647), found 385.1646.

Preparation of 1*D*-(+)-2,4-di-*O*-benzyl-*myo*-inositol (14). The orthoacetate **13** (0.150 g, 0.4 mmol) was dissolved in a mixture of the methanol (3 mL) and 5 M aqueous HCl (3 mL) and refluxed for 5 h. The solvents were removed under reduced pressure and the crude product were purified by column chromatography (by washing the

DOI: 10.1021/acs.cgd.7b00895
Cryst. Growth Des. XXXX, XXX, XXX–XXX

column with ethyl acetate) to isolate the known **14** as a solid (0.130 g, 93%).[22] M.P. 143−145 °C (crystals obtained from *iso*-propanol) Lit. M.P. 145 °C, HPLC analysis showed the enantiomeric purity >99%. R_f = 0.3 (ethyl acetate), Found $[\alpha]_D^{rt}$ (EtOH, *c* = 1.0) = +29.25, Lit $[\alpha]_D^{rt}$ = +29.7 (*c* = 1, EtOH).[22]

RESULTS AND DISCUSSION

The racemic 4-*O*-allyl ethers of *myo*-inositol-1,3,5-orthoesters were prepared by the allylation of the corresponding triol with allyl bromide, in the presence of sodium hydride. Chelation assisted regioselective *O*-alkylation of *myo*-inositol-1,3,5-orthoesters is well precedented in the literature.[23] These racemic allyl ethers were acylated with (−)camphanic acid chloride to obtain a 1:1 mixture of the corresponding diastereomeric dicamphanates (Scheme 1). The postulates and experiments which culminated in the separation of diastereomeric dicamphanates by crystallization and the establishment of the configuration of the individual diastereomers is described below.

Crystallization Behavior of Orthoacetates 7 and dia7. A small quantity of the diastereomeric mixture (0.50 g) of **7** and **dia7** was isolated by rapid column chromatography. Attempts to separate the two diastereomers **7** and **dia7** failed during crystallization from several solvents (acetone, ethanol, methanol, 1,4-dioxane, benzene, toluene, *iso*-propanol, diethyl ether, ethyl acetate, dichloromethane, chloroform). Hence a small quantity of the mixture of diastereomeric allyl ethers (0.50 g) was enriched by flash column chromatography. Both the diastereomers **7** and **dia7** were obtained in about 80% purity (20% being the other diastereomer) as revealed by ^{1}H NMR spectroscopy. The enriched samples were crystallized separately from hot absolute ethanol to yield crystals of the diastereomers **7**·EtOH and **dia7**. There was considerable difference in the solubility of the diastereomeric orthoacetates **7**·EtOH (22 mg/mL) and **dia7** (50 mg/mL) in ethanol. The crystals of the individual diastereomers **7**·EtOH and **dia7** (Figure S10, SI) obtained from ethanol were subsequently used as seed crystals to separate the mixture of the diastereomers on larger scale. Hence the individual diastereomeric orthoacetates **7**·EtOH and **dia7** could be obtained in 45% and 40% yield on 10 g scale, respectively. The purity of both the crystalline diastereomers estimated by HPLC was at least 99%.

We had previously noticed that derivatives of *myo*-inositol orthoesters with comparable molecular structures exhibited similarities in their crystallization behavior and crystal structures.[15−21] The racemic dibenzoates of *myo*-inositol orthoesters in fact crystallized as isomorphs and two of these (racemic 2,4-di-*O*-benzoyl-*myo*-inositol 1,3,5-orthoformate and the corresponding orthoacetate) cocrystallized in closely related space groups.[17] Hence we suspected that the crystallization behavior of diastereomeric orthoformates **8**, **dia8** and orthobenzoate analogs **9**, **dia9** could be similar to that of diastereomeric orthoacetates **7** and **dia7**, allowing their separation by crystallization. The fact that diastereomeric orthoacetates **7** and **dia7** could be separated by crystallization established that they do not cocrystallize, unlike inositol derived diastereomeric camphorsulfonates.[24−26] Hence we thought that diastereomeric orthoformates **8**, **dia8** and orthobenzoates **9**, **dia9** might not form cocrystals and allow their separation by crystallization. Indeed when we prepared and investigated the crystallization behavior and crystal structures of diastereomeric orthoformates **8**, **dia8** and orthobenzoates **9**, **dia9** they did not form cocrystals. Nonformation of cocrystals suggested that the noncovalent interactions between molecules of a given diastereomer (e.g., molecules of **8**) could be stronger than that between molecules of different diastereomers (e.g., molecules of **8** and **dia8**) thus making them amenable for separation by crystallization. All in all, we were able to obtain crystals of five of the six dicamphanates and solve their structures. All the dicamphanates crystallized in chiral space groups as expected (**7**·EtOH - *P*1; **dia8** and **dia9** - $P2_12_12_1$; **dia7**, **8** and **8**·MeOH - $P2_12_12_1$) containing single molecule in the asymmetric unit except **7**·EtOH (Table S1, SI). Crystals of **7**·EtOH contained two molecules in the asymmetric unit along with one molecule of ethanol. Absence of conventional hydrogen bond forming functional groups in these molecules allowed dominance of weaker interactions like C−H···O in their crystals. A comparison of the calculated densities of the diastereomeric pairs revealed slight difference (**7**·EtOH - ethanol solvate, 1.300 g cm^{-3}; **dia7**, 1.269 g cm^{-3}; **8**, 1.339 g cm^{-3}; **8**·MeOH - methanol solvate, 1.368 g cm^{-3}; **dia8**, 1.368 g cm^{-3}; **dia9**, 1.284 g cm^{-3}). The melting point of the diastereomeric orthoformates (**8** and **dia8**) were not very different (the difference was 2−3 °C), but that between crystals of diastereomeric orthoacetates (**7**·EtOH and **dia7**) was significant (45 °C). The ethanol molecules in crystals of **7**·EtOH were retained in the crystal lattice until its melting, which suggested strong association between the constituent molecules in the crystal. The diastereomer **7**·EtOH failed to form a solid in the absence of ethanol, even when cooled to −20 °C indicating the role of ethanol in associating its molecules to yield robust crystals. The orthoformate **8** also formed solvated crystals **8**·MeOH just as the orthoacetate **7** did, with ethanol. But unlike the orthoacetate **7**, orthoformate **8** also crystallized on its own, although these crystals redissolved only to crystallize out as the methanol solvate. The difference in melting points between crystals of **8**·MeOH and **dia8** was about 50−52 °C, but (unlike the orthoacetates) the solvated crystals **8**·MeOH melted at lower temperature and lost methanol on exposure to atmosphere under ambient conditions. However, it was pertinent to note that diastereomers with the same absolute configuration (i.e., **7** and **8**) formed solvated crystals. This is in accordance with our earlier observation that inositol derivatives with similar molecular structure have comparable crystallization behavior. Hence a comparison of the crystal structure of diastereomeric dicamphantes did help us to succeed in the separation of individual diastereomers by crystallization (see below). Crystal structures of **7**·EtOH, **dia7**, **8**, **8**·MeOH, **dia8**, and **dia9** (Figure S96, Figure S98, Figure S99, Figure S104, SI) were compared with a view to correlate the packing of molecules with respect to their separation during crystallization. Short accounts of relevant aspects of the crystal structure of individual diastereomers are given separately.

Orthoformates. A mixture of diastereomers **8** and **dia8** was initially isolated on a small scale (0.700 g) by flash column chromatography. The gummy mixture was triturated with *n*-pentane to obtain a solid. Drop-wise addition of methanol (to the solid−pentane mixture) with warming resulted in a clear solution, which on standing at room temperature for 1 to 2 h deposited very fine needles (Figure S26a-b, SI) of one of the diastereomers (later identified as **8**). These crystals of **8** were subsequently used as seed crystals to separate **8** from a mixture of **8** and **dia8** (on 10 g scale).

The needles of **8** on crystallization from methanol gave blocks of **8** which were unstable at ambient condition and

DOI: 10.1021/acs.cgd.7b00895
Cryst. Growth Des. XXXX, XXX, XXX−XXX

showed loss of crystallinity on exposure to an open atmosphere. Use of a larger proportion of methanol (1:1 pentane−methanol) during the separation of **8** from a mixture of **8** and **dia8**, yielded needles of **8** initially, which redissolved and then crystallized out as the methanol solvate (**8**·MeOH). These crystallization experiments suggested that perhaps the needles of **8** obtained were metastable kinetic crystals, which in the presence of a larger proportion of methanol were transformed to the solvated crystals of **8**. Solution state ^{1}H NMR spectrum of these blocks suggested the ratio of **8** to methanol as 1:1 (Figure S35−39, SI). The presence of methanol in crystals of **8** was also supported by TGA (weight loss of about 5%), DSC (Figures S92−S94, SI), and single crystal X-ray diffraction analysis. Crystals of pure **dia8** for single crystals X-ray diffraction experiments could be obtained by repeated crystallization, but this procedure did not appear to be practical for large scale separation of **dia8**.

Orthobenzoates. A small quantity (0.40 g) of **9** and **dia9** was isolated by rapid column chromatography in order to remove other impurities present in the crude product. Contrary to our expectations, attempts to separate the individual diastereomers by crystallization were not successful. Hence **9** and **dia9** were separated by flash column chromatography. The diastereomer **dia9** could be crystallized from diethyl ether or DMF or *iso*-propanol. The crystals of **dia9** (Figure S52, SI) obtained from *iso*-propanol were subsequently used as seed crystals to separate **dia9** from an *iso*-propanol solution of a mixture of diastereomers (on 5 g scale). Hence **dia9** could be obtained in 20% yield from a mixture of **9** and **dia9** by crystallization. Attempts at crystallization of **9** from common solvents failed; a gummy mass was obtained in all the experiments.

Configuration of chiral diastereomeric orthoesters. The configuration of the diastereomeric orthoformates **8** and the orthobenzoate **dia9** were established by conversion to the corresponding known dicamphanates (Scheme 2).[27,28] The allyl ethers in **8** and **dia9** were cleaved using palladium(II) hydroxide, according to a procedure that we had developed earlier.[29] It is interesting to note that the conditions of cleavage of allyl ethers did not lead to intramolecular migration of the camphanoyl moiety between the C4- and C6-hydroxyl groups in **10** and **11**. These conversions showed **8** and **dia9** to be 1*D*-(+)-2,4-di-*O*-[ω-camphanoyl]-6-*O*-allyl-*myo*-inositol-1,3,5-orthoformate and 1*D*-(−)-2,6-di-*O*-[ω-camphanoyl]-4-*O*-allyl-*myo*-inositol-1,3,5-orthobenzoate, respectively. By default, **dia8** and **9** (both of which could not be obtained pure by crystallization) must be 1*D*-(−)-2,6-di-*O*-[ω-camphanoyl]-4-*O*-allyl-*myo*-inositol-1,3,5-orthoformate and 1*D*-(+)-2,4-di-*O*-[ω-camphanoyl]-6-*O*-allyl-*myo*-inositol-1,3,5-orthobenzoate, respectively.

Scheme 2. Determination of Configuration by Deallylation of 8 and dia9

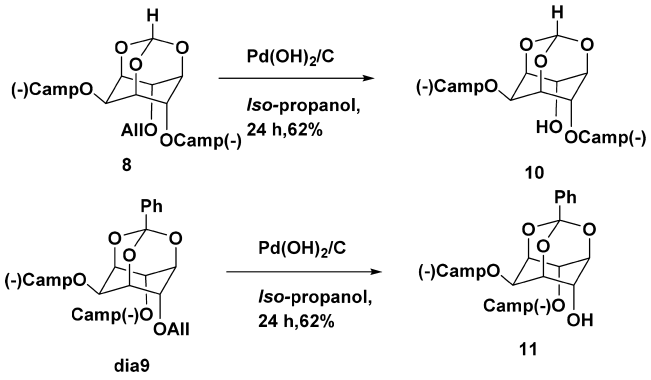

The configuration of the orthoacetates **7**, **dia7** was established by comparison of their single crystal X-ray structures with those of orthoformates **8**, **dia8** (Figure S95, SI). The configuration of **7** and **dia7** could be established by this process since dicamphanates of orthoacetates and orthoformates only differ at the orthoester position, which has no bearing on the absolute configuration of the molecule. Hence **dia7** was found to be 1*D*-(−)-2,6-di-*O*-[ω-camphanoyl]-4-*O*-allyl-*myo*-inositol-1,3,5-orthoacetate and **7** was found to be 1*D*-(+)-2,4-di-*O*-[ω-camphanoyl]-6-*O*-allyl-*myo*-inositol-1,3,5-orthoacetate (Figure S96, SI). The assignment of configuration by a comparison of the single crystal X-ray diffraction data was confirmed by the conversion of both **7** and **dia7** to the known 1*D*-(+)-2,4 and 1*D*-(−)-2,6-di-*O*-benzyl-*myo*-inositol (Scheme 3).

Scheme 3. Conversion of 7 to 1*D*-(+)-2,4-Di-*O*-benzyl-*myo*-inositol (14) and dia7 to 1*D*-(−)-2,6-Di-*O*-benzyl-*myo*-inositol (ent14), Respectively

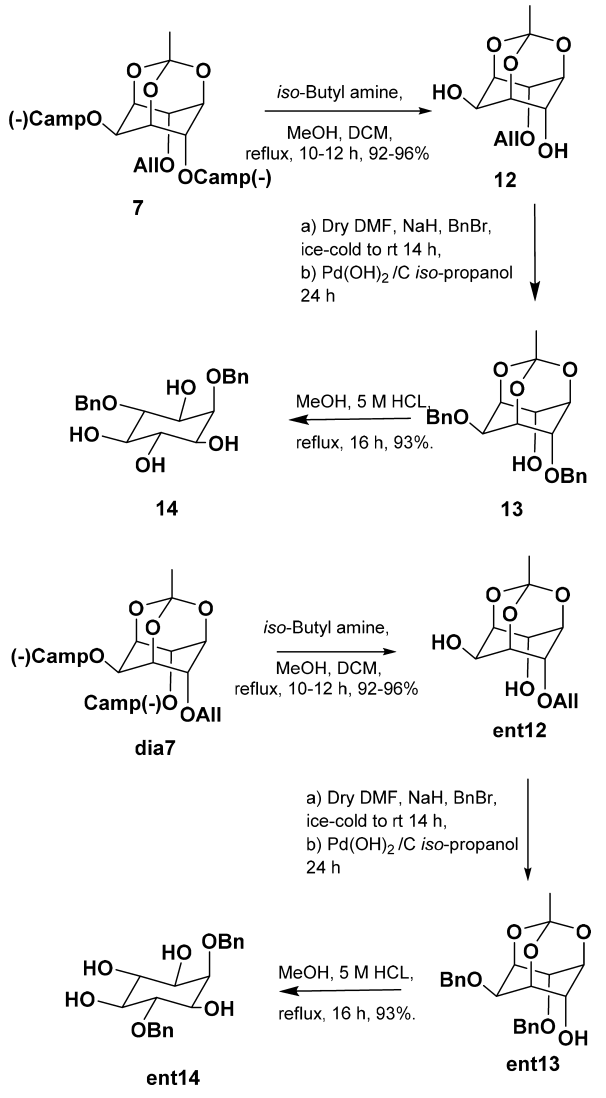

7 **12** **14** **13** **dia7** **ent12** **ent14** **ent13**

DOI: 10.1021/acs.cgd.7b00895
Cryst. Growth Des. XXXX, XXX, XXX−XXX

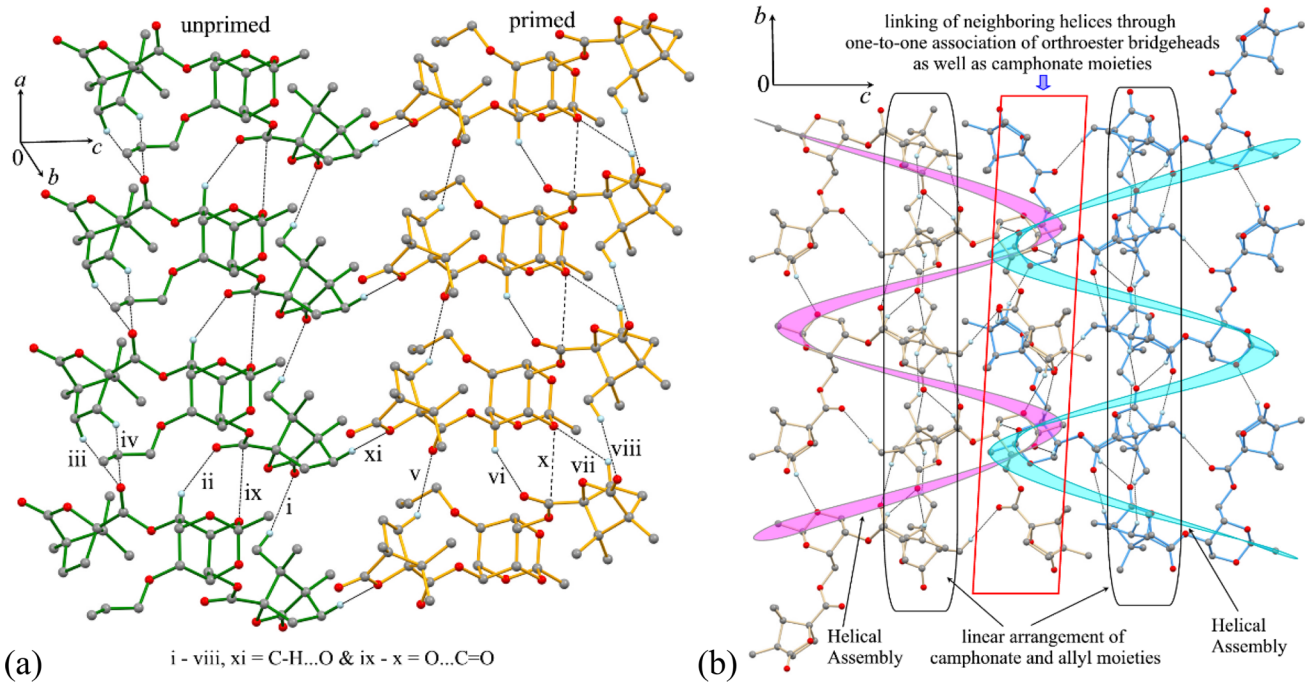

Figure 1. Molecular packing in crystals of (a) 7·EtOH; (b) **dia7** showing columnar and helical assemblies, respectively.

It is pertinent to compare the yield and purity of **14** and **ent14** that we obtained from **7** and **dia7** with the methods reported earlier.[30−34] The yield of **14** and **ent14** in the present work was about 17% starting from *myo*-inositol. In previous reports the yield was between 3% and 46%, but most of these reports involved column chromatography for the separation of the diastereomeric precursors. In the present work, the synthetic sequence involved seven steps and no chromatographic separation of the diastereomers. In two of the previous reports[30,34] yield of one of the diastereomeric ester derivatives obtained was higher than the other, leading to better yield (as compared to the present work) of **ent14**. We suspect that formation of unequal amounts of diastereomeric esters was a result of intramolecular acyl group migration between the C4 and C6 hydroxyl groups. The benzyl ethers **13** and **14** are precursors for *D*-*myo*-inositol-4-phosphate and *D*-*myo*-inositol-1,3,4,5-tetrakisphosphate, resepctively.[34] Our initial attempts to cleave the allyl ether in **dia7**, exclusively, to the corresponding known dicamphanate to establish the configuration of **dia7** was inconclusive. The melting point of the known 1*D*-(−)-2,6-di-*O*-[*ω*-camphanoyl]-*myo*-inositol-1,3,5 orthoacetate was reported to be 228−231 °C, while that of the sample we obtained by allyl ether cleavage of **dia7** was 234−240 °C.[35] Similarly, the dicamphanate obtained by the cleavage of the allyl ether in **7**, had a melting point of 212−215 °C, while the melting point of 1*D*-(+)-2,4-di-*O*-[*ω*-camphanoyl]-*myo*-inositol-1,3,5-orthoacetate was reported to be 201−204 °C.[35] These differences could be due to the intramolecular migration of the camphanoyl moiety between the C4 and C6 hydroxyl groups in the orthoacetate diastereomers, subsequent to the cleavage of the allyl group.

Crystal Structure of 7·EtOH and dia7. Structure overlay of the two symmetry independent molecules in 7·EtOH crystals revealed significant difference in the orientation of allyl groups whereas conformation of camphanate groups were similar (Figure S96, SI). Both symmetry independent molecules (primed and unprimed) generate respective columnar structure through close association of the unit-translated molecules using several C−H···O interactions (Figure 1a) along with short dipolar O···C═O contact[36] with perpendicular motif (Table S2, SI) thereby engaging both camphanate groups and rigid inositol orthoacetate moiety along the shortest axial length (*a*-axis). Both columns along the longer *c*-axis are stitched via a C−H···O interaction involving equatorial C2-*O*-camphanoyl groups to reveal a layered structure on the *ac* plane (Figure S97, SI). Conversely, these adjacent layers have weak association along the *b*-axis. Both symmetry independent molecules together generate a sheet structure on the *bc* plane constructed by an alternate arrangement of primed and unprimed molecules along the *b*-axis. Within the sheet, camphanoyl moieties (C2-equatorial of unprimed and C4-axial of primed) of both symmetry independent molecules are placed alternately to create the helical chain thereby holding the symmetry independent molecules together using C−H···O interactions. Interestingly, the ethanol molecule is mostly associated with unprimed molecules through O−H···O (camphor) hydrogen bond. Ethanol molecule also supplements cohesion of both host molecules through C−H···O contact. Both symmetry independent molecules have a grossly similar packing environment and generate void space in the lattice. The ethanol molecules occupy the void space created between the unprimed molecules, while the allyl moiety of the primed molecule fills the void generated between primed molecules (Figure S97, SI).

Molecules in crystals of **dia7** create a flat helical assembly owing to the crystallographic 2_1-screw axis symmetry relationship in their arrangement (Figure 1b). The helical assembly formed along the *b*-axis mostly engages C6-axial camphanate and allyl groups through C−H···O interactions (Table S3, SI) that place these groups one below the other leading to the generation of linear chain. The helical association is further supplemented by the linking of C2-equatorial camphanate and orthoester bridgehead through C−H···O interactions. Adjacent helices along the *c*-axis are stitched with C−H···O engaging one-to-one association of orthoester and equatorial C2-

DOI: 10.1021/acs.cgd.7b00895
Cryst. Growth Des. XXXX, XXX, XXX−XXX

camphanate moieties resulting in comparatively sparse packing on the *bc* plane.

The computation of packing energies for molecules of **7** in **7**·EtOH crystals and for molecules of **dia7** in their crystal gave the values of ∼ − 238 and −222 kJ mol^{-1}, respectively, indicating that the packing in **7**·EtOH crystals is relatively more robust compared to **dia7** crystals. The intermolecular potential energy values (−94.0 kJ mol^{-1} and −91.4 kJ mol^{-1} for primed and unprimed molecules in **7**·EtOH, respectively) indicated strong association between the molecules along the *a*-axis (Figure 1a), but weaker association between molecules within the sheet structure (with energy values in the range −18.0 to −41.0 kJ mol^{-1}). In contrast, intermolecular potential values between molecules of **dia7** in its crystal were lower (−54.5 kJ mol^{-1} for helix formation and −57.7 kJ mol^{-1} for binding of the helices). Hence intermolecular potential energy calculations suggest relatively stronger affinity between the molecules in **7**·EtOH crystals compared to that between **dia7** molecules in its crystal. These factors rationalize the early formation of **7**·EtOH crystals from the diastereomeric mixture in ethanol solution, resulting in the separation of **7**·EtOH and **dia7**.

Crystal Structures of 8, 8·MeOH, and dia8. Structure overlay of molecules of **8** in solvent free and methanol solvated crystals revealed significant difference in the orientations of both camphanate and allyl moieties indicating different molecular arrangements in their crystals (Figure S99, SI). In solvent free crystals of **8**, closely associated unit-translated molecules generate a linear chain along the *a*-axis through several C−H···O interactions and short dipolar O···C═O contacts having perpendicular motif[37] (Figure 2 and Table S4, SI) involving both camphanate moieties. The neighboring chains along the *a*-axis are tightly linked through head-to-head association of the orthoformate moiety through C−H···O contact (see contact vii in Figure 2). The stitching of the two chains (which are also part of the helix along the crystallographic 2_1-screw axis (*a*-axis, Figure 2) is also supported by the C−H···O (see contact viii in Figure 2). The adjacent helices are loosely associated along the *b*-axis through a C−H···O interaction engaging the camphanate groups of molecules on the *ab* plane (Figure S100, SI). Molecules of **8** are loosely associated down the *a*-axis through C−H···O interactions (Figure S101, SI).

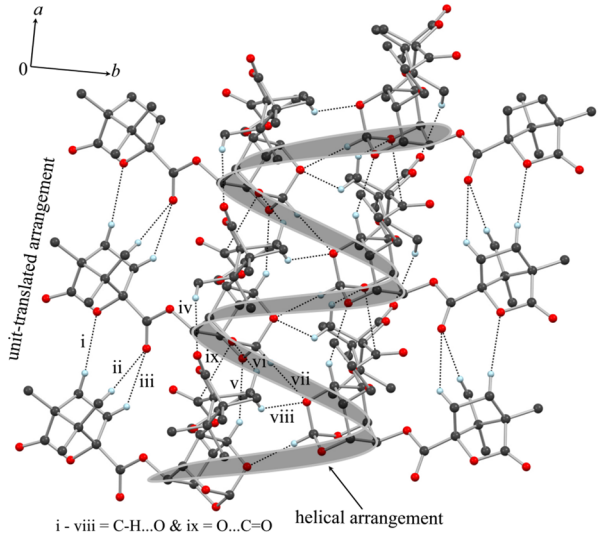

Figure 2. Association of neighboring molecules in a crystal of **8** that generate flat helical structure through C−H···O and dipolar (ether)-O···C═O contacts.

In crystals of **8**·MeOH, neighboring molecules assemble to generate the helical architecture around the crystallographic 2_1 screw axis (Figure 3) through various C−H···O interactions (entries1−5, Table S5, SI). The helical assembly is also supplemented by dipolar C═O···C═O contact[37] of type I motif involving equatorial and axial camphanate groups. The neighboring helices along the *c*-axis are bridged through methanol molecules due to O−H···O and C−H···O hydrogen bonds. Molecules of **8** in **8**·MeOH crystals also assemble helically along the *c*-axis, exclusively through the intervention of methanol molecules (Figure S102, SI).

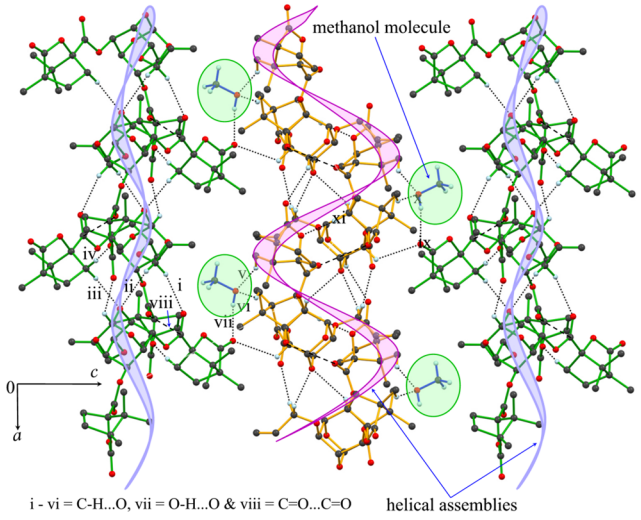

Figure 3. Molecular packing along the *c*-axis showing the association of neighboring helices through methanol molecules in crystals of **8**·MeOH.

In crystals of **dia8**, the closely linked unit-translated molecules generate a linear chain (Figure 4) along the *a*-axis through C−H···O interactions (Table S6, SI) engaging C2-equatorial and C6-axial camphanate moieties with the orthoester and the allyl groups, respectively. The short dipolar (ether) O···C═O contact with perpendicular motif[37] also lends support to the linear assembly along the *a*-axis. The adjoining unit-translated chains along the *c*-axis are held together (Figure 4) through relatively weak C−H···O interaction between the camphanate moieties. Molecular packing viewed down the *a*-axis revealed helical assembly of the molecules along the crystallographic 2_1 screw axis (*b*-axis) using C−H···O interactions. The joining of the adjacent helices along the *c*-axis by another set of C−H···O interactions generate the two-dimensional corrugated structure (Figure S103, SI).

The computation of packing energies for **8**, **8**·MeOH, and **dia8** gave the values of ∼ −235.5 kJ mol^{-1}, − 271.66 kJ mol^{-1}, and −240.0 kJ mol^{-1}, respectively, indicating that the packing in **8**·MeOH crystals is relatively more robust compared to **8** and **dia8** crystals. These values are consistent with dissolution of initially formed crystals of **8** and formation of the solvated crystals **8**.MeOH. The estimation of intermolecular potential energy values in solvent free crystals of **8** revealed higher value (−93.2 kJ mol^{-1}) for helical association of molecules (Figure 2) as compared to that for linking of these helices (−34.6 and

DOI: 10.1021/acs.cgd.7b00895
Cryst. Growth Des. XXXX, XXX, XXX−XXX

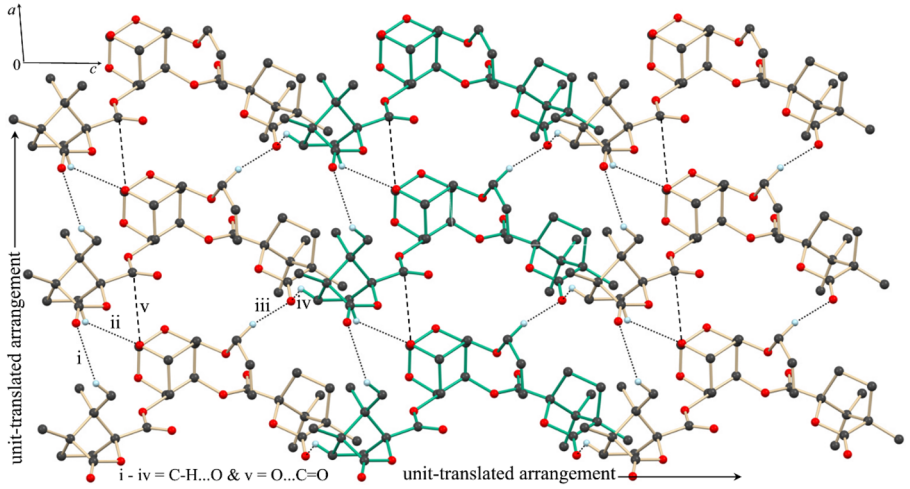

Figure 4. Molecular packing in crystals of **dia8** showing linking of the linear chains through C−H···O interactions.

−38.9 kJ mol^{-1}). This weak association would have led to its dissolution in methanol to yield more robust methanol solvate **8**·MeOH. The intermolecular potential energy value (−90.8 kJ mol^{-1}) for the generation of the helical chain in **8**·MeOH crystals (Figure 3) through cohesion of orthoester-bridge is similar to that in crystals of **8**, but the affinity between molecules of methanol and **8** leads to the formation of **8**·MeOH crystals. The intermolecular potential energy values for the linear association of molecules to form chains and association of these chains in crystals of **dia8** were found to be −87.7 kJ mol^{-1} and −40 kJ mol^{-1}, respectively. Hence it appears that the ability of molecules of **8** to form solvated crystals contributes to the separation of **8** and **dia8** from their solution. This aspect is similar to that observed during the separation of **7** and **dia7**.

Crystal Structure of the Orthobenzoate dia9. Molecules of **dia9** generate a flat helical assembly (Figure 5) through C−H···O interactions across the crystallographic 2_1-screw axis (*b*-axis) (entry 1, Table S7, SI). The helical architecture also places the unit-translated molecule of the helix in close association through several C−H···O interactions and short dipolar C═O···C═O contact of type I motif[37] involving the carbonyl group of both camphanate moieties. The computation of packing energy for **dia9** gave a value of ∼ −244.7 kJ mol^{-1}. The estimation of the intermolecular potential value revealed a higher energy value (−86.2 kJ mol^{-1}) for unit-translated association of molecules within helices but the intermolecular potential energy value for linking of molecules along the crystallographic 2_1-screw axis (−15.6 kJ mol^{-1}) as well as for the linking of the helices along the *c*-axis (−14.5 kJ mol^{-1}) were low (Figure S105, SI). However, intermolecular potential value for the linking of the neighboring chains along the *a*-axis via short and linear C−H···O contacts (Figure S106, SI) was relatively high (−57.5 kJ mol^{-1}).

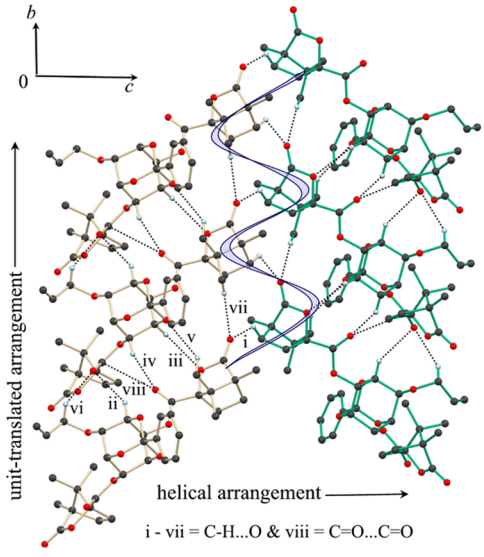

Figure 5. Molecular packing viewed down the *a*-axis in crystals of **dia9** showing helical assembly of molecules.

CONCLUSIONS

In the last 2−3 decades the increase in the pace of reporting of crystals structures has swelled the crystal structure database considerably. However, instances of the analysis and use of crystal structure data to aid organic synthesis are very limited. We recently showed that the crystal structure database can be used for the identification of molecular crystals that could undergo intermolecular acyl transfer reactions.[38] The present work illustrates that crystallization procedures for the separation of diastereomers could be evolved due to the knowledge of the crystal structures of inositol derivatives of comparable molecular structure. The packing energies and intermolecular potential values estimated from crystal structures correlate well with the process of separation of diastereomers during crystallization. Hence the results presented here raises the hope that crystal structure database could facilitate organic synthesis.

Synthetic implications of the present work are that we have developed a convenient and practical method for the preparation of chiral protected *myo*-inositol derivatives without involving laborious chromatographic methods of separation. The chiral derivatives can be obtained in gram quantities and the methods are amenable to further scale-up due to the simple procedures involved. Although molecular structure of orthoformate, orthoacetate, and orthobenzoate derivatives of *myo*-inositol are similar, the difference in substitution (H, methyl, phenyl) at the apical orthoester position makes a world of difference during the hydrolytic and the reductive cleavage of these orthoesters. These differences in product formation can

DOI: 10.1021/acs.cgd.7b00895
Cryst. Growth Des. XXXX, XXX, XXX−XXX

be exploited for the synthesis of different cyclitol derivatives, and this has been reviewed.[3] Hence we are hopeful that the results presented here fills in the lacuna in using the abundantly available *myo*-inositol as a starting material for the synthesis of chiral phosphoinositols, cyclitols, and their derivatives as well as natural products and their analogs containing these moieties.

■ ASSOCIATED CONTENT

Supporting Information

The Supporting Information is available free of charge on the ACS Publications website at DOI: 10.1021/acs.cgd.7b00895.

Experimental details for the preparation and separation of **8**, **dia8**, **9**, **dia9**, **10**, and **11**; spectral data; thermal analysis data; and crystal structure data (PDF)

Accession Codes

CCDC 1551163−1551168 contain the supplementary crystallographic data for this paper. These data can be obtained free of charge via www.ccdc.cam.ac.uk/data_request/cif, or by emailing data_request@ccdc.cam.ac.uk, or by contacting The Cambridge Crystallographic Data Centre, 12 Union Road, Cambridge CB2 1EZ, UK; fax: +44 1223 336033.

■ AUTHOR INFORMATION

Corresponding Authors

*E-mail: ms.shashidhar@ncl.res.in. Phone: 91-20-25902055. Fax: 91-20-25902629.

*E-mail: rg.gonnade@ncl.res.in. Phone: 020-25902225. Fax: 020-25902642.

ORCID

Mysore S. Shashidhar: 0000-0002-8477-1149

Rajesh G. Gonnade: 0000-0002-2841-0197

Author Contributions

The manuscript was written through contributions of all authors. All authors have given approval to the final version of the manuscript.

Funding

This work was made possible by financial support from Science and Engineering Research Board, Department of Science and Technology, New Delhi (grant number SB/S1/OC-23/2013), New Delhi.

Notes

The authors declare no competing financial interest.

■ ACKNOWLEDGMENTS

NTP and MIT thank CSIR, India for a research fellowship. This work was supported by the Science and Engineering Research Board, New Delhi (grant number SB/S1/OC-23/2013).

■ REFERENCES

(1) Hancock, J. T. *Cell Signalling*; Oxford University Press: New Delhi, India, 2005.

(2) Balla, T. *Physiol. Rev.* **2013**, *93*, 1019−1137.

(3) Gurale, B. P.; Sardessai, R. S.; Shashidhar, M. S. *Carbohydr. Res.* **2014**, *399*, 8−14.

(4) Thomas, M. P.; Mills, S. J.; Potter, B. V. L *Angew. Chem., Int. Ed.* **2016**, *55*, 1614−1650.

(5) Painter, G. F.; Grove, S. J. A.; Gilbert, I. H.; Holmes, A. B.; Raithby, P. R.; Hill, M. L.; Hawkins, P. T.; Stephens, L. R. *J. Chem. Soc., Perkin Trans. 1* **1999**, *8*, 923−936.

(6) Murali, C.; Shashidhar, M. S.; Gopinath, C. S. *Tetrahedron* **2007**, *63*, 4149−4155.

(7) Murali, C.; Gurale, B. P.; Shashidhar, M. S. *Eur. J. Org. Chem.* **2010**, *4*, 755−764.

(8) Wessig, P.; Mollnitz, K.; Hubner, S. *Synlett* **2010**, *10*, 1497−1500.

(9) Jagdhane, R. C.; Shashidhar, M. S. *Eur. J. Org. Chem.* **2010**, *15*, 2945−2953.

(10) Sureshan, K. M.; Shashidhar, M. S.; Varma, A. J. *J. Org. Chem.* **2002**, *67*, 6884−6888.

(11) Dixit, S. S.; Shashidhar, M. S.; Devaraj, S. *Tetrahedron* **2006**, *62*, 4360−4363.

(12) Gurale, B. P.; Shashidhar, M. S.; Gonnade, R. G. *J. Org. Chem.* **2012**, *77*, 5801−5807.

(13) Mondal, S.; Sureshan, K. M. *Org. Biomol. Chem.* **2014**, *12*, 7279−7289.

(14) Praveen, T.; Samanta, U.; Das, T.; Shashidhar, M. S.; Chakrabarti, P. *J. Am. Chem. Soc.* **1998**, *120*, 3842−3845.

(15) Gonnade, R. G.; Bhadbhade, M. M.; Shashidhar, M. S. *Chem. Commun.* **2004**, *22*, 2530−2531.

(16) Gonnade, R. G.; Bhadbhade, M. M.; Shashidhar, M. S.; Sanki, A. K. *Chem. Commun.* **2005**, *47*, 5870−5872.

(17) Sarmah, M. P.; Gonnade, R. G.; Shashidhar, M. S.; Bhadbhade, M. M. *Chem. - Eur. J.* **2005**, *11*, 2103−2110.

(18) Murali, C.; Shashidhar, M. S.; Gonnade, R. G.; Bhadbhade, M. M. *Chem. - Eur. J.* **2009**, *15*, 261−269.

(19) Krishnaswamy, S.; Gonnade, R. G.; Shashidhar, M. S.; Bhadbhade, M. M. *CrystEngComm* **2010**, *12*, 4184−4197.

(20) Sardessai, R.; Krishnaswamy, S.; Shashidhar, M. S. *CrystEngComm* **2012**, *14*, 8010−8016.

(21) Krishnaswamy, S.; Shashidhar, M. S.; Bhadbhade, M. M. *Cryst. Growth Des.* **2017**, *17*, 117−126.

(22) Laumen, K.; Ghisalba, O. *Biosci., Biotechnol., Biochem.* **1999**, *63*, 1374−1377.

(23) Devaraj, S.; Shashidhar, M. S.; Dixit, S. S. *Tetrahedron* **2005**, *61*, 529−536.

(24) Manoj, K.; Sureshan, K. M.; Gonnade, R. G.; Bhadbhade, M. M.; Shashidhar, M. S. *Cryst. Growth Des.* **2005**, *5*, 833−836.

(25) Manoj, K.; Gonnade, R. G.; Shashidhar, M. S.; Bhadbhade, M. M. *CrystEngComm* **2012**, *14*, 1716−1722.

(26) Manoj, K.; Gonnade, R. G.; Bhadbhade, M. M.; Shashidhar, M. S. *Cryst. Growth Des.* **2006**, *6*, 1485−1492.

(27) Riley, A. M.; Mahon, M. F.; Potter, B. V. L *Angew. Chem., Int. Ed. Engl.* **1997**, *36*, 1472−1474.

(28) Riley, A. M.; Godage, H. Y.; Mahon, M. F.; Potter, B. V. L *Tetrahedron: Asymmetry* **2006**, *17*, 171−174.

(29) Mart, A.; Shashidhar, M. S. *Tetrahedron* **2012**, *68*, 9769−9776.

(30) Baudin, G.; Glänzer, B. I.; Swaminathan, K. S.; Vasella, A. *Helv. Chim. Acta* **1988**, *71*, 1367−1378.

(31) Watanabe, Y.; Akinori, O.; Yasushi, S.; Ozaki, S. *Tetrahedron Lett.* **1990**, *31*, 2613−2616.

(32) Sureshan, K. M.; Shashidhar, M. S.; Praveen, T.; Gonnade, R. G.; Bhadbhade, M. M. *Carbohydr. Res.* **2002**, *337*, 2399−2410.

(33) Sureshan, K. M.; Watanabe, Y. *Tetrahedron: Asymmetry* **2004**, *15*, 1193−1198.

(34) Watanabe, Y.; Nakahira, H.; Bunya, M.; Ozaki, S. *Tetrahedron Lett.* **1987**, *28*, 4179−4180.

(35) Garrett, S. W.; Liu, C.; Riley, A. M.; Potter, B. V. L *J. Chem. Soc., Perkin Trans. 1* **1998**, *8*, 1367−1368.

(36) Manoj, K.; Gonnade, R. G.; Bhadbhade, M. M.; Shashidhar, M. S. *CrystEngComm* **2009**, *11*, 1022−1029.

(37) Allen, F. H.; Baalham, C. A.; Lommerse, J. P. M.; Raithby, P. R. *Acta Crystallogr., Sect. B: Struct. Sci.* **1998**, *54*, 320−329.

(38) Tamboli, M. I.; Krishnaswamy, S.; Gonnade, R. G.; Shashidhar, M. S. *Chem. - Eur. J.* **2013**, *19*, 12867−12874.

DOI: 10.1021/acs.cgd.7b00895
Cryst. Growth Des. XXXX, XXX, XXX−XXX